



Kinetics and mechanism of hydrogenation of furfural on Cu/SiO₂ catalysts

Surapas Sitthisa^a, Tawan Sooknoi^a, Yuguang Ma^c, Perla B. Balbuena^{c,d}, Daniel E. Resasco^{a,b,*}

^a School of Chemical, Biological, and Materials Engineering, University of Oklahoma, Norman, OK 73019, USA

^b Center for Biomass Refining, University of Oklahoma, Norman, OK 73019, USA

^c Department of Chemical Engineering, Texas A&M University, College Station, TX 77843, USA

^d Materials Science and Engineering Program, Texas A&M University, College Station, TX 77843, USA

ARTICLE INFO

Article history:

Received 17 July 2010

Revised 28 September 2010

Accepted 8 October 2010

Available online 12 November 2010

Keywords:

Aldehyde hydrogenation

Copper catalyst

Reaction kinetics

DRIFTS

DFT calculations

ABSTRACT

The hydrogenation/hydrodeoxygenation of furfural was studied on a Cu/SiO₂ catalyst at 230–290 °C. Detailed kinetics, density function (DFT) calculations, and spectroscopic studies were combined to investigate this reaction. A Langmuir–Hinshelwood model was found to fit the kinetic data well and provided the parameters of physical significance. The heat of adsorption (ΔH_{ads}) of furfural, derived from the fitting, was found to be significantly higher than those of furfuryl alcohol and 2-methyl furan. Activation energies for the conversion of furfural and furfuryl alcohol were both about 12 kcal/mol. DFT calculations and DRIFTS provided guidance about the nature of the surface species. Accordingly, the most likely species adsorbed on the Cu surface is suggested to be a top $\eta^1(O)$ -aldehyde. DFT calculations of the reaction path show that the predicted energy barriers are of the same order as the experimental values and suggest that the hydrogenation of furfural can occur via either an alkoxide or ahydroxyalkyl intermediate.

© 2010 Elsevier Inc. All rights reserved.

1. Introduction

In most of the approaches being investigated for the production of biofuels, furfurals appear as important intermediates [1]. For example, furfural is directly obtained by the acid-catalyzed dehydration of xylose, the main building block of hemicellulose, one of the constituents of biomass. Furfurals are also present in bio-oil obtained from the fast pyrolysis of biomass [2,3]. This brown viscous liquid contains many oxygenated compounds that impart unwanted properties to the oil, making it unsuitable as a transportation fuel [4–12]. Due to the high reactivity of these compounds, it is necessary to catalytically upgrade bio-oil in order to improve its storage stability, boiling point range, water solubility, and octane number. Mild hydrogenation is one of the potential routes for bio-oil stabilization, which eliminates the most reactive oxygenate groups, which in turn are the least desirable in fuel components [13,14].

The present contribution focuses on the study of furfural conversion as a model compound of biomass-derived feedstocks [15–25]. As opposed to Pd, on which decarbonylation is the dominant conversion path [26,27], Cu is highly selective for the

hydrogenation of furfural to furfuryl alcohol, with methyl furan only appearing at temperatures >200 °C [28].

The exact reaction pathway by which the carbonyl group in the aldehyde gets hydrogenated is not fully understood. For example, it has been proposed that the first step is the formation of a C–H bond, yielding an alkoxide intermediate, which is then followed by the addition of the second H atom to this intermediate, forming an adsorbed alcohol [29]. Alternatively, it is also possible that the first step might involve the addition of H to the O atom, thus forming a hydroxylalkyl intermediate, which subsequently would yield the adsorbed alcohol [30,31].

In this work, we examine both mechanisms for the case of furfural on Cu surfaces, which has not been previously investigated. We have investigated the kinetics and reaction pathways of furfural-aldehyde hydrogenation over a silica-supported Cu catalyst. These studies have been complemented with DFT calculations of adsorbed furfural on Cu(1 1 1) and Cu(1 1 0) planes, as well as DRIFTS analysis of adsorbed furfural species conducted on unsupported Cu metal powder, to avoid adsorption on the support that masks the signal from the metal. DFT calculations and DRIFTS have helped us identify the type of adsorbed species on the Cu surface and explore the reaction pathways involved in the conversion of furfural. Understanding the chemistry of the aldehyde functional group on Cu surfaces may have a broader impact on the study of other deoxygenation reactions involved in the refining of biomass-derived oils.

* Corresponding author at: Center for Biomass Refining, University of Oklahoma, Norman, OK 73019, USA. Fax: +1 405 325 5813.

E-mail address: resasco@ou.edu (D.E. Resasco).

2. Methodology

2.1. Catalyst synthesis and characterization

A 10 wt.% Cu/SiO₂ catalyst was prepared by incipient wetness impregnation (IWI). A 1.5 M Cu(NO₃)₂ (Fluka, 99.9%) aqueous solution was added to the silica support (SiO₂, Hisil) at a liquid/solid ratio of 1 cc/g. After impregnation, the catalyst was dried overnight at room temperature and then placed in an oven at 120 °C for 12 h. The oven-dried catalyst was finally calcined for 4 h at 400 °C following a linear heating ramp of 10 °C/min, under the flow of pure air at 100 ml/min.

Several physical/chemical techniques were employed to characterize the Cu/SiO₂ catalyst. Morphology and size of the Cu clusters present in the catalyst were characterized by transmission electron microscopy (TEM). The BET surface area (S_g) was measured by N₂ physisorption in a Micromeritics ASAP 2010 unit.

The reducibility of calcined sample was determined by temperature-programmed reduction (TPR). For these measurements, 50 mg of calcined catalyst was placed in a quartz tube, heated at 10 °C/min under 20 ml/min of He up to 550 °C, and held at the temperature for 1 h. The sample was then cooled down to 30 °C and exposed to a stream of 5% H₂/Ar with the flow rate of 20 ml/min. After that, it was heated to 600 °C with a ramping rate of 10 °C/min. The amount of hydrogen consumed as a function of temperature was monitored online by a TCD detector. The fraction of Cu reduced was estimated from the H₂ consumption experiment, using a known amount of CuO for calibration.

2.2. Reaction kinetics

The vapor-phase reaction of furfural over Cu/SiO₂ was conducted in an isothermal tubular reactor, and the data were analyzed assuming an isothermal integral plug flow reactor (PFR). The pelletized catalyst (size range: 250–425 μm) was placed at the center of a vertical tubular quartz reactor between two layers of glass beads and quartz wool. Calculations were done to ensure that external and internal mass transfer limitations were eliminated following the criteria proposed by Madon and Boudart [32]. The catalyst was pre-reduced in the flow of H₂ (60 ml/min, Airgas, 99.99%) for 1 h at 350 °C. After reduction, the catalyst was cooled down to the selected temperature (230–290 °C) under the same H₂ flow rate. A 0.5 ml/h flow of liquid furfural (Aldrich, 99.5%) was fed continuously from a syringe pump (Cole Palmer) and vaporized into a gas stream of 60 ml/min H₂. The reaction products were analyzed online by a gas chromatograph (Agilent model 6890) using an HP-5 capillary column and a FID detector. The carbon balance was checked in every run, and it was found to be better than 95% in each case. Pure furfural, pure furfuryl alcohol, and an equimolar mixture of the two were used as feeds. To examine the effects of water on reaction rates, in some runs, the H₂ gas was saturated with water at 40 °C.

A rate expression that includes the concentrations of furfuraldehyde, furfuryl alcohol, and 2-methyl furan, based on the conventional Langmuir–Hinshelwood mechanism, was used to fit the experimental results. Nonlinear least-square regression analysis of the differences between the experimental values and the calculated values was used to simultaneously fit the data for several temperatures and several initial feed compositions. To ensure that the fitting resulted in the global minimum, we tried different initial guesses of the adjustable parameters to make sure that the program always converged to the same minimum with the same fitting parameters for the different initial guesses. This

simultaneous fitting of different runs at different temperatures and over a wide range of concentrations using a single set of kinetics parameters illustrates the goodness of the rate expression. The validity of the fitting parameters was further tested by a set of additional reaction runs, in which mixture feeds with different proportions were used. The experimental yields obtained with these mixtures were compared with the values predicted from the model obtained from the initial set of runs.

2.3. Infrared absorption spectroscopy of furfural adsorbed on Cu metal

Diffuse reflectance infrared Fourier transformation (DRIFT) spectra of adsorbed furfural were recorded in a high temperature DRIFT cell (HVC, Harrick) with CaF₂ windows. The Cu sample powder (100 mg) was loaded in the sample cup of the cell, reduced *in situ* at 500 °C for 1 h under a flow of H₂ (30 ml/min), and then purged with He (30 ml/min) for 30 min. Finally, the sample was cooled down to room temperature, and the background spectrum was recorded. A He carrier gas (30 ml/min) saturated at 0 °C with furfural vapor was passed by the cell for approximately 30 min. The sample was then purged under He flow at room temperature for another 30 min. The DRIFT spectra were recorded at a resolution of 4 cm⁻¹ and accumulating 256 scans.

2.4. Density functional theory calculations

Spin-polarized periodic DFT calculations were made using the Vienna *ab initio* simulation package (VASP) [33–37], in which the Kohn–Sham equations are solved by self-consistent algorithms. The valence electrons were described by plane wave basis sets with a cutoff energy of 300 eV, and the core electrons were replaced by the projector augmented wave (PAW) pseudo-potentials [38,39] for improving the computational efficiency. The Brillouin zone was sampled with a 4 × 4 × 1 Monkhorst–Pack *k*-point mesh. The exchange–correlation functional was described within the generalized gradient approximation (GGA) proposed by Perdew, Burke, and Ernzerhof (PBE) [40]. The Methfessel–Paxon method was employed to determine electron occupancies with a smearing width of 0.2 eV.

Both Cu(111) and Cu(110) slab models were constructed based on a 5 × 5 unit cell. The Cu(111) slab model consists of three metal layers and seven equivalent vacuum layers (>16 Å); the Cu(110) slab is also composed of three metal layers, with a ~18 Å vacuum gap in the direction perpendicular to the surface. The lattice constant of the face-centered cubic (fcc) Cu from our bulk calculation, 3.626 Å, was in good agreement with the experimental value of 3.610 Å [41]. The two uppermost layers of the slab were allowed to relax to their lowest energy configuration, while the atoms of the bottom layer were fixed to the bulk positions, keeping their optimized lattice constants. The slab model was relaxed until the forces were convergent to 0.01 eV/Å.

Surface adsorption takes place on the topmost layer of the slab. Three adsorption types for furfural molecules, named parallel-ring modes, perpendicular-ring modes, and single-site adsorption modes, were examined. All adsorbate atoms were allowed to relax to their optimized positions. The adsorption energy, E_{ads} , is given by the following equation

$$E_{ads} = E_{slab/ads} - E_{slab} - E_{gas}$$

in which $E_{slab/ads}$ is the total energy of the slab with adsorbates, E_{slab} is the energy of the slab, and E_{gas} is the energy of the adsorbates in gas phase. For the hydrogenation reactions, the minimum energy

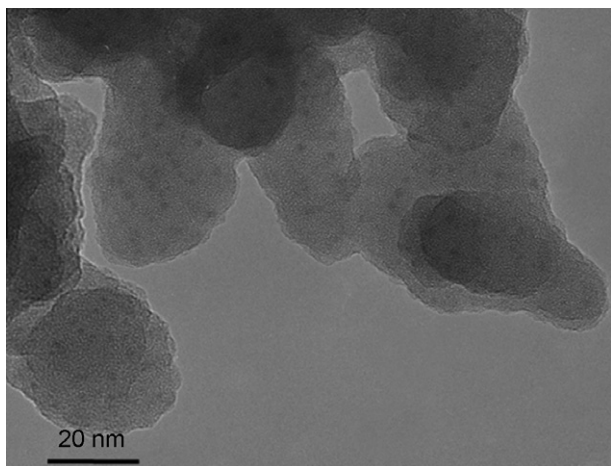


Fig. 1. TEM micrograph of the 10% Cu/SiO₂ catalysts, showing ~3- to 4-nm Cu clusters dispersed on the silica support particles (~50 nm).

paths, transition states (TS), and energy barriers were determined by the nudged elastic band (NEB) method [42,43].

3. Results

3.1. Cu/SiO₂ catalyst characterization

A typical TEM image of the Cu/SiO₂ catalyst is presented in Fig. 1. It can be seen that the metallic copper clusters are well dispersed on the silica support, with an average particle size of ~3 nm. Estimated Cu dispersion (based on TEM Cu cluster size), Cu content, and BET total surface area of the catalyst are reported in Table 1. As shown in the TPR profile of Fig. 2, the maximum rate of H₂ consumption was observed at about 350 °C. Therefore, complete reduction of Cu can be expected after a pre-reduction treatment conducted in pure H₂ at 350 °C for 1 h.

3.2. Furfural reaction over Cu/SiO₂

No deactivation was observed in any of the catalytic activity runs during 4 h of steady-state conversion. However, to compare the runs under identical conditions, a fresh catalyst was used in each separate experiment. In agreement with a previous report [44], the reaction of furfural (FAL) on Cu/SiO₂ gives mainly furfuryl alcohol (FOL), with 2-methyl furan (MF) as a minor product, which is significant only above 230 °C. As shown in Fig. 3, 2-methyl furan is clearly a secondary product of the aldehyde (i.e. zero derivative at low W/F in Fig. 3a), but a primary product of the conversion of the alcohol (i.e., non-zero derivative at low W/F in Fig. 3b). Therefore, it is apparent that furfural is first converted into furfuryl alcohol, and the deoxygenation only occurs from the alcohol. As shown in Fig. 3a, at high W/F, the yield of furfuryl alcohol reaches a plateau as the aldehyde/alcohol equilibrium conversion is approached. Similarly, a plateau in furfural formation is reached at high W/F when the feed is pure furfuryl alcohol (Fig. 3b). However, no decarbonylation product was observed at any temperature of the range in this investigation. In summary, from this simple analysis, the reaction pathway can be described as follows:

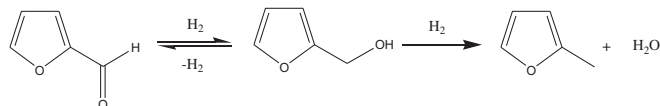


Table 1
Properties of the 10 wt.% Cu/SiO₂ catalyst.

Cu average particle diameter	3.2 ± 0.2 nm
Cu dispersion from TEM	40 ± 2.5%
BET surface area	110 ± 10 m ² /g
Catalyst particle size	250–425 μm
Cu metal content	10.3 wt.%

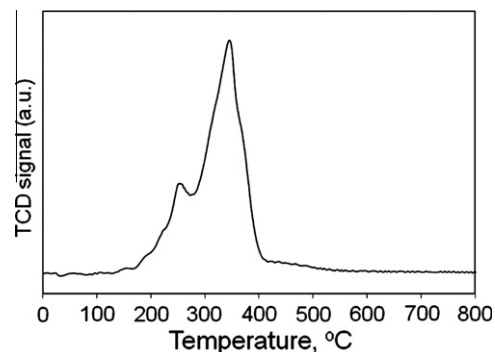


Fig. 2. Temperature-programmed reduction (TPR) of 10 wt.% Cu/SiO₂ catalyst.

3.3. Kinetics of furfural deoxygenation

From the reaction pathway proposed above, a rate expression based on the conventional Langmuir–Hinshelwood kinetic model was derived, with the following assumptions [45,46]:

- (i) molecular adsorption of furfural (FAL), furfuryl alcohol (FOL), and 2-methyl furan (MF),
- (ii) dissociative adsorption of hydrogen,
- (iii) all adsorption sites are equivalent and independent of coverage, and
- (iv) surface reaction is the rate-determining step.

Accordingly, the elementary steps for furfural conversion can be described by the following equations, in which * represents an active site.



Since in excess of hydrogen, the partial pressure of hydrogen can be considered constant during the entire reaction period, the rate expressions become:

$$r_{\text{FAL}} = -k_1 \theta_{\text{FAL}} + k_{-1} \theta_{\text{FOL}} \quad (8)$$

$$r_{\text{FOL}} = k_1 \theta_{\text{FAL}} - k_{-1} \theta_{\text{FOL}} - k_2 \theta_{\text{FOL}} \quad (9)$$

$$r_{\text{MF}} = k_2 \theta_{\text{FOL}} \quad (10)$$

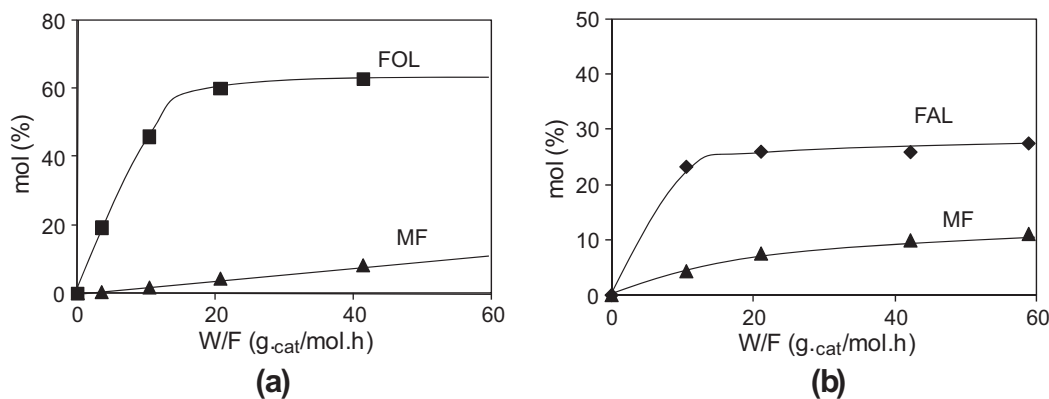


Fig. 3. Yield of products from the reaction of (a) furfural (FAL) and (b) furfuryl alcohol (FOL) over 10 wt.%Cu/SiO₂. Temp. = 290 °C, H₂/feed ratio = 25, H₂ pressure = 1 atm, TOS = 15 min.

where θ_{FAL} is the fractional coverage of furfural, θ_{FOL} the fractional coverage of furfuryl alcohol, and θ_{MF} the fractional coverage of 2-methyl furan.

$$\theta_{FAL} = K_{FAL}P_{FAL}\theta_V \quad (11)$$

$$\theta_{FOL} = K_{FOL}P_{FOL}\theta_V \quad (12)$$

$$\theta_{MF} = K_{MF}P_{MF}\theta_V \quad (13)$$

$$\theta_H = K_H^{1/2}P_{H_2}^{1/2}\theta_V \quad (14)$$

Using the conventional LH kinetics derivation, the rate expressions become:

$$r_{FAL} = -k_1K_{FAL}P_{FAL}\theta_V + \frac{k_1}{K}K_{FOL}P_{FOL}\theta_V \quad (15)$$

$$r_{FOL} = k_1K_{FAL}P_{FAL} - \left[\frac{k_1}{K}K_{FOL}P_{FOL}\theta_V + k_2K_{FOL}P_{FOL}\theta_V \right] \quad (16)$$

$$r_{2-MF} = k_2K_{FOL}P_{FOL}\theta_V \quad (17)$$

$$\theta_V = \frac{1}{1 + K_{FAL}P_{FAL} + K_{FOL}P_{FOL} + K_{MF}P_{MF} + K_H^{1/2}P_{H_2}^{1/2}} \quad (18)$$

The results of the fitting of the experimental concentrations of furfural, furfuryl alcohol, and 2-methyl furan as a function of space time (W/F) with the kinetic model derived from these equations are shown in Figs. 4–6 for the feeds of furfural, furfuryl alcohol, and an equimolar mixture of furfural and furfuryl alcohol, respectively. A very satisfactory agreement between the kinetic model and the experimental data was obtained over the entire range of W/F and temperatures. Only a slight discrepancy has been observed in the prediction of 2-methyl furan, which seems to be slightly higher than the experimental measurement.

The equilibrium (K_{eq}) and kinetic (k_i) constants obtained from the fitting at three different temperatures are shown in Table 2. As expected, since K_{eq} represents the equilibrium constant for the exothermic furfural hydrogenation reaction, it decreases with temperature. The corresponding heat of reaction (ΔH), calculated by substituting the equilibrium constants in the Van't Hoff equation, was 11.9 kcal/mol. All the kinetic rate constants (k_i) increase with temperature and the Arrhenius plots (see Fig. 7a) yield straight lines, from which true activation energies are readily obtained. The corresponding values were of 11.8 kcal/mol and 12.4 kcal/mol for the hydrogenation of furfural (E_1) and the hydrodeoxygenation of furfuryl alcohol (E_2), respectively. These values are also in line with those reported for the same reactions conducted over a

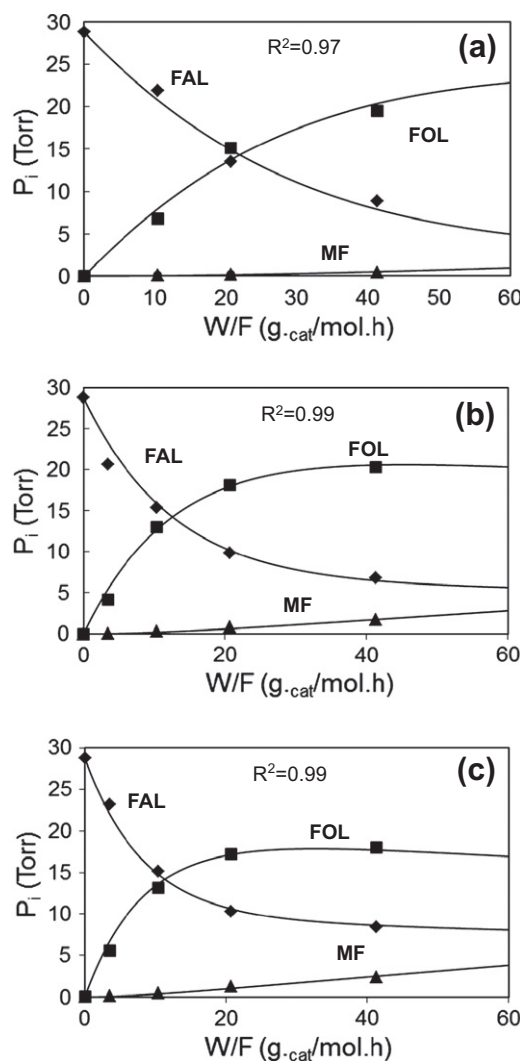


Fig. 4. Partial pressures of the reactant and products from the reaction of furfural on the 10 wt.%Cu/SiO₂ catalyst at: (a) 230 °C, (b) 270 °C and (c) 290 °C. The points are experimental data and the lines are calculated from the kinetics model.

copper chromite catalyst [47] and, as shown below, agree well with those predicted from DFT calculations.

The equilibrium adsorption constants (K_i) can be readily derived from the fittings. The K_i values shown in Table 2 decrease with

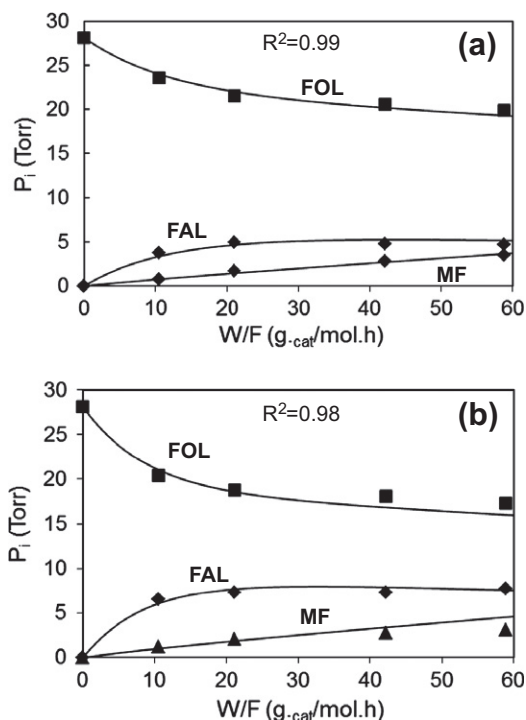


Fig. 5. Partial pressures of the reactant and products from the reaction of furfuryl alcohol on the 10 wt.%Cu/SiO₂ catalyst at: (a) 270 °C and (b) 290 °C. The points are experimental data, and the lines are calculated from the kinetics model.

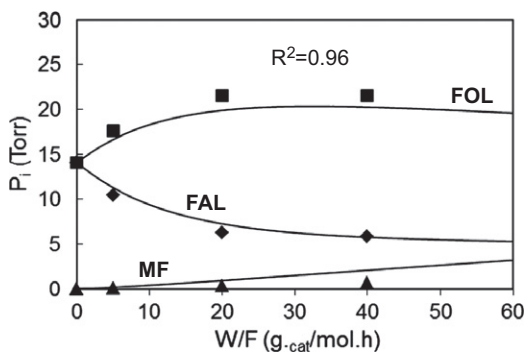


Fig. 6. Partial pressures of the reactant and products from the reaction of a mixture of 50 mol% furfural and 50 mol% of furfuryl alcohol on the 10 wt.%Cu/SiO₂ catalyst at 270 °C. The points are experimental data, and the lines are calculated from the kinetics model.

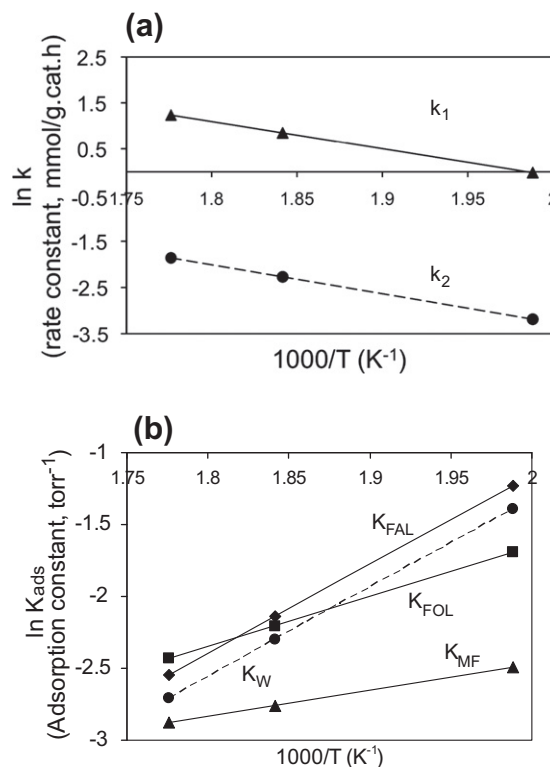


Fig. 7. Rate constants, k_i , (a) and adsorption equilibrium constants, K_{ads} , (b) as a function of inverse temperature.

increasing temperature, as expected. Accordingly, the $\ln K_i$ vs. $1/T$ plots (Fig. 7b) can be used to estimate the heat of adsorption for all the species involved, according to the Van't Hoff equation. In line with previous reports [46], the values of K_{H_2} are relatively small in comparison with the other K_i on Cu catalyst. From these plots, the heat of adsorption of hydrogen on Cu/SiO₂ was determined to be 13.9 kcal/mol, which is in excellent agreement with those reported in the literature [45,46]. The heat of adsorption of furfural (12.3 kcal/mol) is shown to be higher than that of furfuryl alcohol (6.9 kcal/mol). In agreement with these estimates, Rioux and Vannice [46] reported that the heat of adsorption of carbonyl-containing molecules on copper (aldehyde/ketone) is significantly higher than that of molecules containing the C–OH group (alcohol). More interestingly, the kinetically derived heat of adsorption of 2-methyl furan (3.7 kcal/mol) on Cu is dramatically lower than that of furfural and even close to a heat of physisorption. As discussed below, the DFT calculations clearly show that the strongest interaction of furfural with the Cu surface is via the

Table 2

Kinetic and thermodynamic parameters obtained from fitting the experimental data of with the kinetic model at various temperatures.

Temp. (°C)	Equilibrium constant			Rate constant (mmol/g cat h)		Adsorption constant (Torr ⁻¹)				
	(K_{eq})			k_1	k_2	K_{FAL}	K_{FOL}	K_{MF}	K_{H_2}	K_W
230	4.56			3.00	0.10	0.29	0.18	0.083	11.9×10^{-5}	0.25
270	2.98			5.93	0.24	0.12	0.11	0.063	4.2×10^{-5}	0.10
290	2.01			8.05	0.34	0.08	0.09	0.056	2.7×10^{-5}	0.07
ΔS_{ads} (cal mol ⁻¹ K ⁻¹)					S_g (cal mol ⁻¹ K ⁻¹)					
FAL	FOL	MF	H ₂	H ₂ O	FAL	FOL	MF	H ₂ ⁺	H ₂ O ⁺	
-13.8	-4.0	-1.0	-32.9	-14.2	-	-	-	-34.1	47.4	

^a From Ref. [52].

carbonyl oxygen. However, the furan ring is not strongly bound to the surface, but rather it exerts a repulsion that increases with the surface density of Cu atoms. This behavior contrasts with that of other metals such as Pd or Pt, which can strongly bind the furan ring [27,48,49].

The validity of the kinetic model and fitting parameters was tested with additional reactions runs, in which mixtures of furfuraldehyde, furfuryl alcohol, and 2-methyl furan were fed in different proportions. Without changing any of the fitting parameters obtained in the original fitting, the experimental yields obtained with the mixtures were compared with the values predicted from the model. As shown in Fig. 8, excellent agreement between the predicted values and the experimental data was obtained in each of the additional runs.

The kinetic model and all the associated parameters were also valid for predicting the reaction of furfural in the presence of water (at a H₂O/FAL ratio of 20 mol/mol). To account for the effect of water coverage (θ_w), a new term was included in the denominator of the kinetics model. By only fitting the new term in the kinetic model, K_w , but without modifying any of the other parameters obtained previously, the fitting was entirely in agreement with the experimental results, as shown in Fig. 9. To test the robustness of the model, we allow the rest of the kinetic parameters vary

simultaneously with the variation of the water terms. Regardless of the initial conditions chosen for the fitting, the results were the same (within 0.1%), with only the new water term parameter changing with respect to the case of the water-free runs. This result indicates that water competes with the other species for adsorption sites without changing the equilibrium parameters (i.e. K_i 's) of the other species. That is, the original kinetic model and all the associated parameters were valid for predicting the reaction of FAL in the presence of water. The resulting equilibrium adsorption constant of water (K_w) varied from 0.249 to 0.067 as the temperature varied from 230 to 290 °C. The linear plot of $\ln K_w$ vs. $1/T$ in Fig. 7b was used to obtain a heat of adsorption of 12.4 kcal/mol for water on Cu/SiO₂. As the heat of adsorption of water is relatively high, the competitive adsorption of water with furfuraldehyde molecule on the Cu surface can be expected to lower the conversion, as seen in Fig. 10. However, in agreement with the rate expression, the effect of water was less pronounced at high temperature, despite the high concentration of water in the vapor phase. Vannice [50] has recommended a set of criteria to validate the thermodynamic parameters extracted from kinetic fittings. The ΔS_{ads} must be negative, and it must be in absolute value smaller than the standard entropy in the vapor phase. The calculated ΔS_{ads} values for all species, as derived from the fittings, are

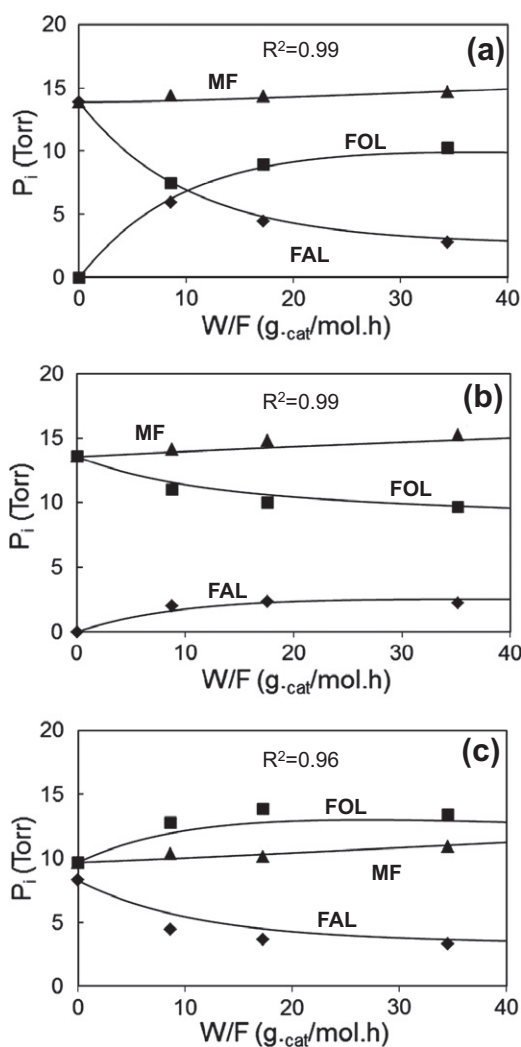


Fig. 8. Partial pressures of the reactant and products from the reaction of the following mixtures: (a) 50% FAL – 50% MF, (b) 50% FOL – 50% MF, (c) 30% FAL – 35% FOL – 35% MF.

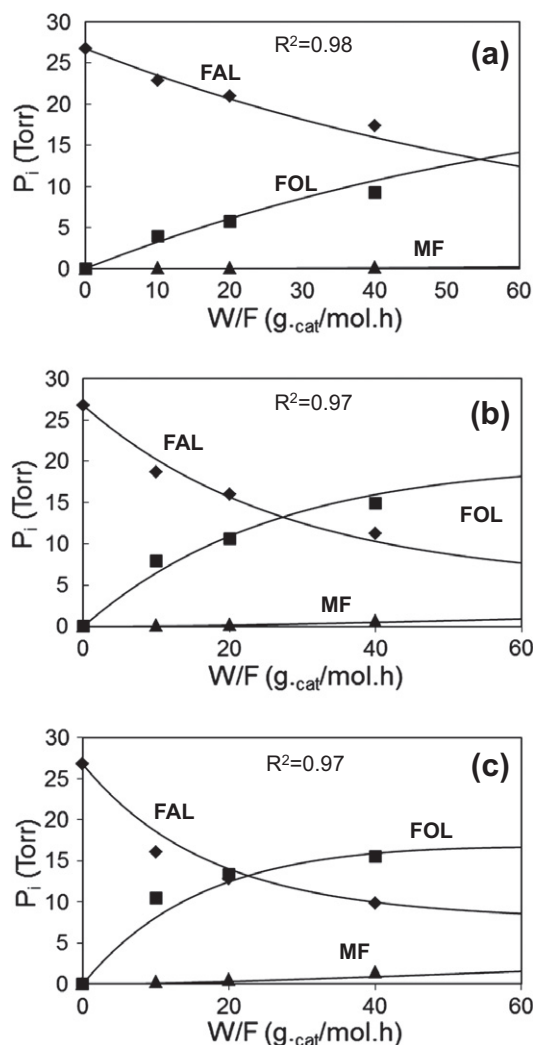


Fig. 9. Partial pressures of the reactant and products from the reaction of furfural in the presence of water at: (a) 230 °C, (b) 270 °C and (c) 290 °C. Feed mole composition-furfural:water, 1:20. The points are experimental data and the lines are calculated from the kinetics model.

summarized in Table 2. The calculated entropy change for adsorption of each one of the species obtained from the intercept in the Van't Hoff plot is negative and complies with the criteria $0 < -\Delta S_{ads} < S_g$ [50,51]. The ΔS_{ads} values for water ($-14.2 \text{ cal mol}^{-1} \text{ K}^{-1}$) and for hydrogen ($-32.9 \text{ cal mol}^{-1} \text{ K}^{-1}$) adsorption were lower than the value of the absolute gas-phase entropy [52]. The values for gas-phase entropy (S_g) for FAL, FOL, and MF were not available for comparison, but reported values for similar compounds (e.g. isopropanol, acetone) range between 65 and $75 \text{ cal mol}^{-1} \text{ K}^{-1}$ [46], significantly higher than the $-\Delta S_{ads}$ values obtained from the fittings. It is interesting to compare the rather high ΔS_{ads} value of $32.4 \text{ cal mol}^{-1} \text{ K}^{-1}$ for hydrogen on Cu relative to that of hydrogen on Pd ($28.9 \text{ cal mol}^{-1} \text{ K}^{-1}$) [53] and gas-phase S_g value of $34.1 \text{ cal mol}^{-1} \text{ K}^{-1}$ [52]. The conclusion would be that H atoms should be quite mobile on the Cu surface.

3.4. DRIFT spectra of furfural adsorbed on Cu

Barbeau and co-workers have extensively investigated the nature of surface species during the adsorption of aldehydes on different metals [54–57]. They have shown that, depending

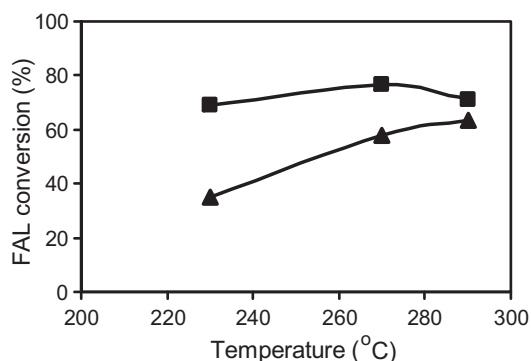


Fig. 10. Conversion of furfural over 10 wt.%Cu/SiO₂. Feed: pure furfural (◆); furfural with water (▲). Temp. = 290 °C, H₂/feed ratio = 25, H₂ pressure = 1 atm, TOS = 15 min.

on the type of metal surface and reaction conditions, aldehydes tend to form surface intermediates, in which either only the carbonyl O is adsorbed atop a metal atom, i.e. $\eta^1(\text{O})$, or both C and O interact with the surface, i.e. $\eta^2(\text{C,O})$. For example, they have shown that while the $\eta^2(\text{C,O})$ state is preferred on clean Pd surfaces, the $\eta^1(\text{O})$ state is preferred when oxygen is present [55,56].

In this work, we have conducted DRIFT spectroscopy to elucidate the nature of the most abundant surface aldehydes on Cu. On a high surface-area-supported catalyst, such as Cu/SiO₂, furfural-aldehyde mainly adsorbs on the surface of silica [58], as seen by the decrease in the intensity of the silanol group band ($-\text{Si}-\text{OH}$, 3740 cm^{-1}) [59] and the rising of a broad band at 3450 cm^{-1} due

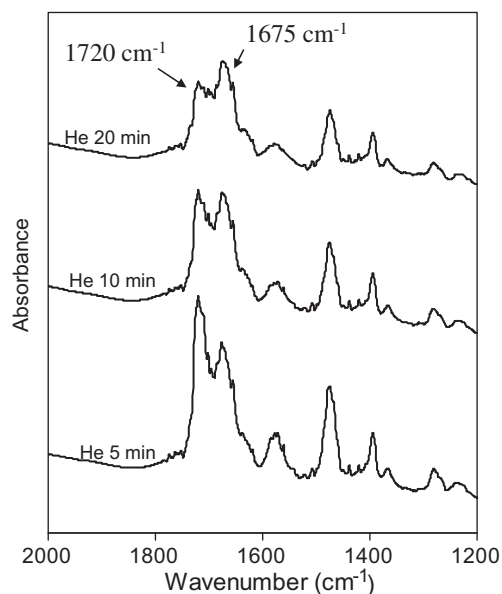


Fig. 12. DRIFT spectra of furfural adsorbed on pure Cu metal powder at 30 °C after pretreatment in H₂ at 350 °C for 1 h.

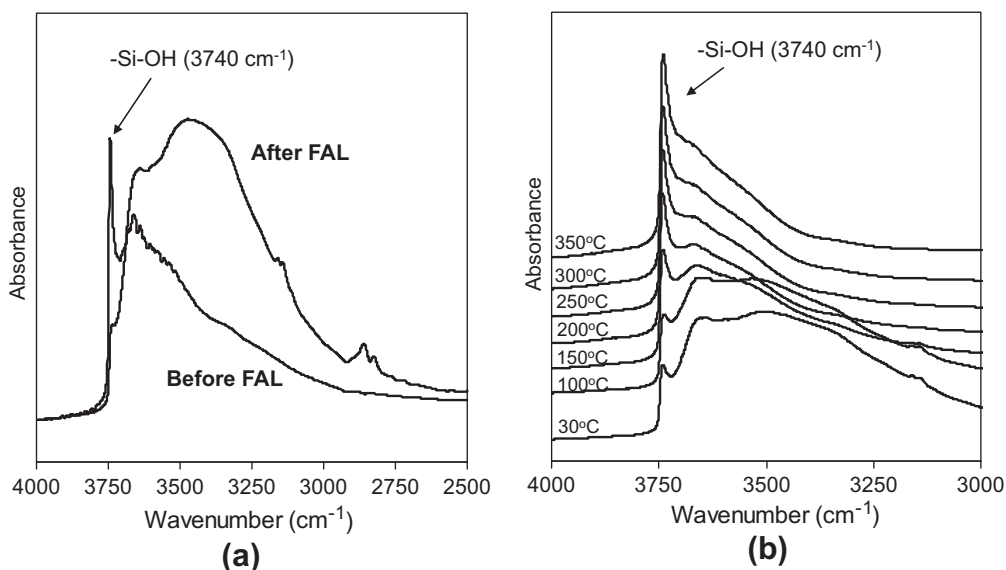


Fig. 11. DRIFT spectra of 10 Cu/SiO₂ at 30 °C recorded before and after adsorption of furfural (a) and at increasing temperatures following adsorption.

to the interaction of silanol with furfural (Fig. 11a). The silanol group band can be recovered by increasing the temperature to 400 °C (Fig. 11b). Therefore, due to the strong interaction between furfural and silica, the adsorption of furfural on Cu cannot be clearly observed. Therefore, to eliminate the effect of the support, pure copper metal was used.

Gas-phase furfural shows the C=O stretching vibration mode at 1720 cm^{-1} along with the C–H stretching band of the aldehydic hydrogen at 2700 cm^{-1} and 2800 cm^{-1} . As shown in Fig. 12, the C–O stretching band in the adsorbed furfural species appears at around 1670 cm^{-1} , downshifted from the wavenumber observed for gas-phase furfural. This lower frequency indicates a weakening of the C–O bond as a result of the interaction with the surface [60,61], but only through an interaction with the carbonyl O, that is $\eta^1(\text{O})$. Formation of a bi-coordinated $\eta^2(\text{C},\text{O})$ surface species would result in a much larger downshift, i.e., below wavenumbers of 1450 cm^{-1} [62].

3.5. DFT calculations

3.5.1. Adsorption of furfural on Cu(1 1 1)

Calculating the adsorption of furfural on Cu(1 1 1) is complex because of its numerous plausible adsorption modes, and it could be even more complicated if intermolecular interactions of furfural molecules are taken into account. In order to neglect intermolecular interactions of adsorbed molecules on the Cu(1 1 1) surface, we choose a low-coverage surface (1/25 ML) by setting a relatively large unit cell (5×5). The furfural contains two O atoms, one in the carbonyl and one in the aromatic ring. According to our DFT calculations, the distance between these two atoms, which are the possible adsorption points in the furfural molecule, is 2.809 Å (in the gas phase). This distance is comparable to the distance between the centers of two hollow sites or between one top and one hollow site (2.96 Å) on the Cu(1 1 1) surface, as shown in Fig. 13. Accordingly, we suppose that the oxygen atoms are located on

Table 3
Calculated bond lengths (Å), bond angles (°), and surface adsorption energies (kcal/mol), E_{ads} , for furfural adsorption on Cu(1 1 1).

Geometry	E_{ads}	d_1	d_2	d_3	d_4	d_5	d_6	d_7	θ
Gas		1.229	1.458	1.395	1.367	1.377	1.424	1.389	124.6
1	8.30	1.280	1.439	1.397	1.396	1.402	1.416	1.412	125.0
2	7.61	1.280	1.438	1.396	1.382	1.396	1.419	1.409	124.8
3	11.53	1.294	1.432	1.400	1.408	1.413	1.417	1.415	122.9
4	1.38	1.259	1.441	1.389	1.370	1.380	1.417	1.395	126.3
5	9.45	1.288	1.449	1.401	1.377	1.386	1.435	1.407	121.5
6	11.53	1.299	1.438	1.395	1.401	1.409	1.407	1.411	126.9
7	−3.00	1.259	1.433	1.389	1.365	1.383	1.419	1.382	123.0
8	−3.46	1.257	1.433	1.391	1.366	1.383	1.425	1.383	123.7
9	1.38	1.263	1.425	1.394	1.368	1.379	1.422	1.393	124.6
10	2.77	1.253	1.436	1.388	1.363	1.381	1.422	1.394	124.1
11	0.69	1.255	1.433	1.392	1.366	1.375	1.424	1.396	123.9
12	−1.15	1.250	1.427	1.394	1.377	1.374	1.420	1.391	127.8
13	0.69	1.255	1.432	1.390	1.374	1.375	1.422	1.389	126.9
14	0.46	1.251	1.431	1.391	1.369	1.377	1.423	1.389	126.9
15	−3.92	1.251	1.429	1.392	1.370	1.379	1.424	1.389	128.1

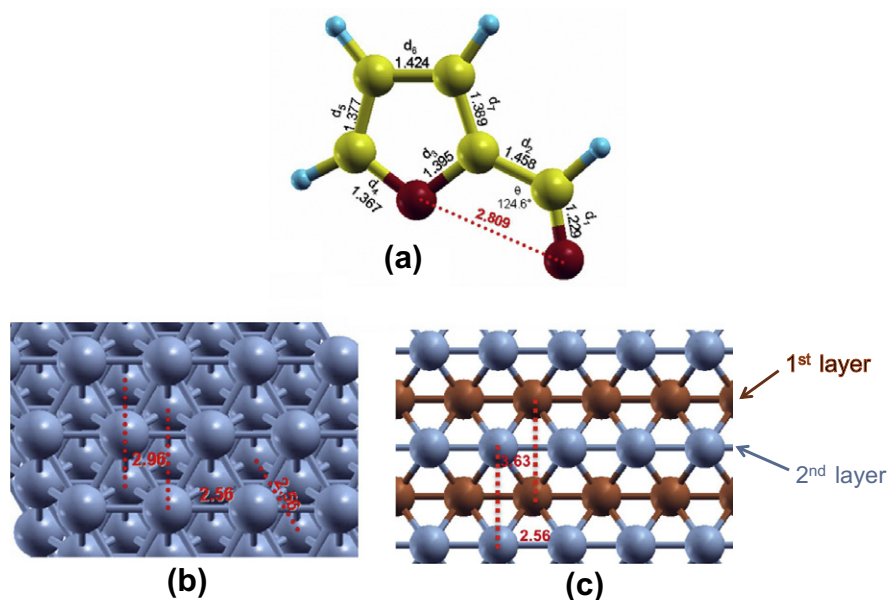


Fig. 13. (a) DFT optimized geometry of furfural in gas phase. Red, yellow, and light blue spheres represent oxygen, carbon, and hydrogen atoms, respectively. (b) DFT optimized surface layer geometry of Cu(1 1 1) slab. (c) DFT optimized surface layer geometry of Cu(1 1 0) slab. Cu atoms on top layer are denoted by bluish gray spheres, and those in the second layer are denoted by brown spheres. Bond angles, bond lengths, and some important distances (Å) are labeled. (For interpretation of the references to colour in this figure legend, the reader is referred to the web version of this article.)

top and/or hollow sites. Plausible adsorption configurations of furfural are thus constructed and can be classified into three types: (a) parallel-ring adsorption: the furfural molecule is roughly parallel to the surface; (b) carbonyl adsorption: the C=O bond is involved in the interaction with the surface; and (c) perpendicular adsorption: the furfural molecule is approximately perpendicular to the Cu(1 1 1) surface. Fifteen initial geometries investigated by our DFT calculations were compared (see Table 3).

Our calculations show that none of the parallel-ring configurations (structures 1–6 in Table 3) are stable on Cu(1 1 1). The adsorption energies range from 1.38 to 11.53 kcal/mol. The carbonyl oxygen atom is ~ 2.0 – 2.1 Å from the metal surface, indicating a strong interaction between the O and Cu atoms. Nevertheless, these adsorption modes destabilize the aromatic furan ring structure. Compared to the geometry in the gas phase (Fig. 13), the bond lengths d_4 , d_5 , and d_7 are elongated in the adsorption state, while d_6 is slightly shortened (Table 3). In general, the weakened aromatic bonds raise the total energy of the adsorbed molecule, leading to a positive (endothermic) adsorption energy. Moreover, the bond length of C=O, d_1 , is 0.03–0.07 Å longer in the parallel mode, mainly due to the interaction between O and the surface.

The perpendicular-ring mode (structures 9–15) shows stronger surface adsorption than the parallel-ring one. The values of E_{ads} range from 3.92 to 2.77 kcal/mol. Only two configurations, 12 and 15, possess negative adsorption energy. Two possible points for adsorption in the furfural molecule are the carbonyl oxygen atom and the ring oxygen atom. The optimized geometries show that the carbonyl O is closer to the Cu(1 1 1) surface compared to the ring O, suggesting that the interaction between the carbonyl O and the Cu(1 1 1) surface is the main contributor to the adsorption. In general, a short carbonyl O-surface distance results in strong surface adsorption. Since the 3d band of the surface Cu atoms partially overlaps the anti-bonding orbital of the aromatic ring, the ring O–Cu surface interaction may reduce the binding strength. This is confirmed by comparing the adsorption energy of two similar configurations (12 and 15): Configuration 15 has a stronger binding strength ($E_{ads} = -3.92$ kcal/mol) but a much longer ring O-surface distance (3.08 Å), corresponding to a weaker ring O-surface interaction. Moreover, the carbonyl O-surface distance in the perpendicular configurations is comparable to that in the parallel configurations. The stronger surface adsorption in the perpendicular-ring mode can be attributed to the approximately unchanged structure of the aromatic furan ring.

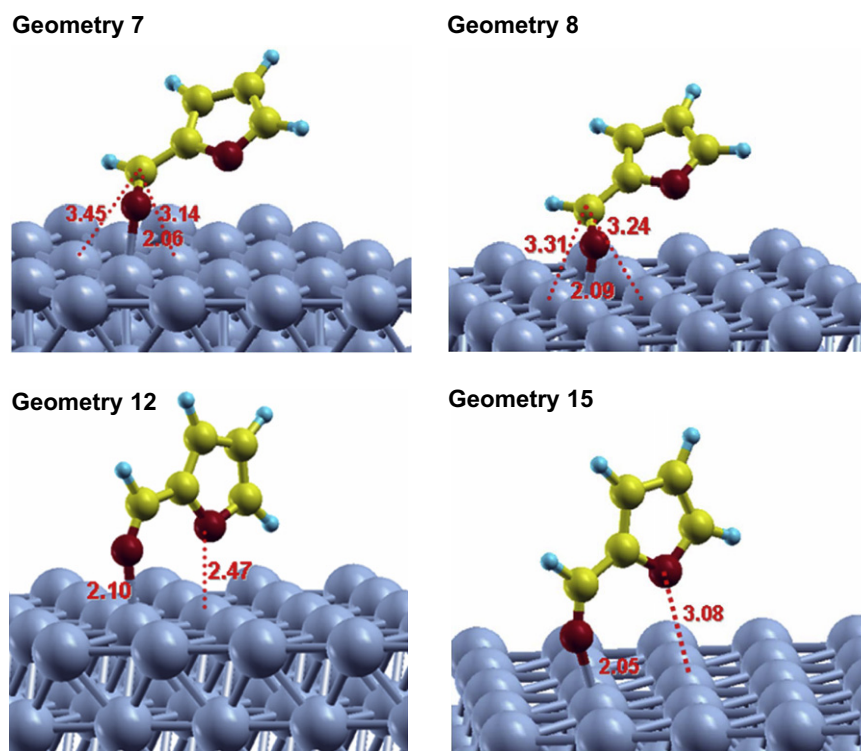


Fig. 14. Optimized geometries for adsorption configuration on Cu(1 1 1) with higher adsorption energies. The distances shown in the figure are in Å. For other plausible geometries, see Supplementary data.

Table 4

Calculated bond lengths (Å), bond angles ($^\circ$), and surface adsorption energies (kcal/mol), E_{ads} , for furfural adsorption on Cu(1 1 0).

Geometry	E_{ads}	d_1	d_2	d_3	d_4	d_5	d_6	d_7	θ
Gas		1.229	1.458	1.395	1.367	1.377	1.424	1.389	124.6
1	-2.77	1.283	1.420	1.410	1.428	1.413	1.406	1.410	123.9
2	-4.84	1.283	1.438	1.389	1.369	1.382	1.421	1.394	122.7
3	-7.38	1.249	1.438	1.392	1.366	1.379	1.422	1.392	125.6
4	-5.07	1.255	1.434	1.398	1.373	1.375	1.423	1.395	128.3
5	-5.07	1.259	1.436	1.392	1.366	1.380	1.418	1.398	126.4

Our calculations reveal that the initial carbonyl configurations, in which both the C and O atoms interact with the surface are not stable on Cu(1 1 1). It is observed that the carbonyl C atom moves away from the Cu(1 1 1) surface after energy optimization. Consequently, the binding strength solely depends on the carbonyl O–Cu interaction. This adsorption mode (structures 7 and 8 in Fig. 14) is determined as the most stable. For the top–top and top-bridge geometries, the calculated adsorption energies are -2.99 to -3.46 kcal/mol, respectively. The top-bridge geometry, 8, is slightly more stable than the top–top geometry.

3.5.2. Adsorption on Cu(1 1 0)

As shown in Fig. 13, the Cu(1 1 0) surface has higher rugosity and is not as close-packed than Cu(1 1 1). This configuration may lessen the repulsion of the furan ring when the carbonyl O approaches the surface. Consequently, more stable binding of furfuraldehyde molecules is expected on Cu(1 1 0) than on Cu(1 1 1), on which interaction with the aromatic ring was found unfavorable. Analogous to the adsorption on Cu(1 1 1), the adsorption configurations can also be roughly divided into parallel, carbonyl, and perpendicular modes. We select five typical geometries to examine their respective adsorption behavior on a low-coverage Cu(1 1 0) surface (1/25 ML), including one parallel configuration, one carbonyl adsorption configuration, and three perpendicular configurations.

The adsorption of furfural is stable for all five configurations. The calculated adsorption energy varies from -2.77 kcal/mol to -7.38 kcal/mol, which are stronger than those on the Cu(1 1 1) surface. The geometric parameters are summarized in Table 4: a longer C=O bond (d_1) and a shorter C–C bond (d_2), primarily arising from the carbonyl O–surface interaction, are found in the adsorbed furfural molecule. In the parallel-ring configuration, the furan ring has the closest distance to the surface, corresponding to the weakest binding strength on Cu(1 1 0) ($E_{ads} = -2.77$ kcal/mol), in line with the repulsion effects seen in the case of Cu(1 1 1). The adsorption, however, is still stronger than the parallel-ring mode on Cu(1 1 1), because less Cu atoms are involved in the interaction with the aromatic ring on the (1 1 0) surface. The distortion of the ring structure is also observed and the general trend is similar to that on Cu(1 1 1), with elongated bond lengths, $d_3, d_4, d_5,$ and d_7 , and a shortened bond length d_6 . Comparing with the carbonyl adsorption on Cu(1 1 0) and that on Cu(1 1 1), we notice significant difference between them: The carbonyl C atom shows a tendency to stay away from the Cu(1 1 1) surface, whereas it gets much closer to the Cu(1 1 0) surface. The C–Cu and O–Cu distances are 2.39 and 2.01 Å, respectively. The discrepancy can be attributed to the different structures of Cu(1 1 1) and

Cu(1 1 0). The furfural molecule is inclined to keep a planar structure owing to the conjugation effect. Cu(1 1 0), as a sparse surface, is able to bind the carbonyl C atom and to keep the planar structure as well (Fig. 15). The close-packed Cu(1 1 1) surface, however, cannot allow the carbonyl C adsorption and the planar furfural structure simultaneously. The calculated adsorption energy (-4.84 kcal/mol) indicates a little stronger binding strength on Cu(1 1 0). Among the perpendicular configurations, 3 is found to be the most stable one ($E_{ads} = -7.38$ kcal/mol), because of the relatively long distance of the ring atoms and the surface (Fig. 15). In configurations 4 and 5 (not shown), the furan ring comes nearer to the (1 1 0) surface and the additional adsorption sites weaken the binding strength due to the same reason described in the previous section.

3.5.3. Hydrogenation of furfural on Cu(1 1 1)

A mechanism for the hydrogenation of propanal and acetone has been proposed [29], in which hydrogenation of the carbonyl group first takes place on the C atom, leading to an alkoxide intermediate. In the following step, addition of a second hydrogen atom to the alkoxide intermediate yields an alcohol. An alternative mechanism is also possible [30,31], in which hydrogenation occurs in the first step at the carbonyl O atom with formation of a hydroxylalkyl intermediate, followed by addition of the second hydrogen atom to form furfuryl alcohol. In this work, first, we examine both mechanisms on Cu(1 1 1) and aim at comparing their similarity and differences using configuration 8 (Table 3).

Dihydrogen dissociation yields adsorbed hydrogen atoms on the metal surface, and the most stable adsorption site is determined as fcc hollow according to our calculations. We therefore suppose the hydrogen atoms are located on the fcc site initially. The detailed geometries of the adsorbed furfural molecules, their transition states, and intermediates are given in Fig. 16 for mechanisms (a) and (b). In mechanism (a), a weak surface adsorption of furfural is observed: The distance between the surface and the carbonyl O is 2.50 Å. The adsorbed H atom located below the furfural molecule moves toward the carbonyl C atom in the process. The energy barrier of this step is 10.84 kcal/mol. The geometry of the transition state is similar to the alkoxide intermediate, suggesting an endothermic reaction. The bond length of C=O increases from 1.25 Å to 1.39 Å, indicating that the bond is significantly weakened and partially converted to a single bond. The alkoxide species is strongly adsorbed by the metal surface with a short Cu–O distance of 1.94 Å, as the unpaired electron on the O atom forms a bond with the Cu(1 1 1) surface.

Analogous to mechanism (a), the formation of the hydroxylalkyl intermediate is also an endothermic reaction in mechanism (b),

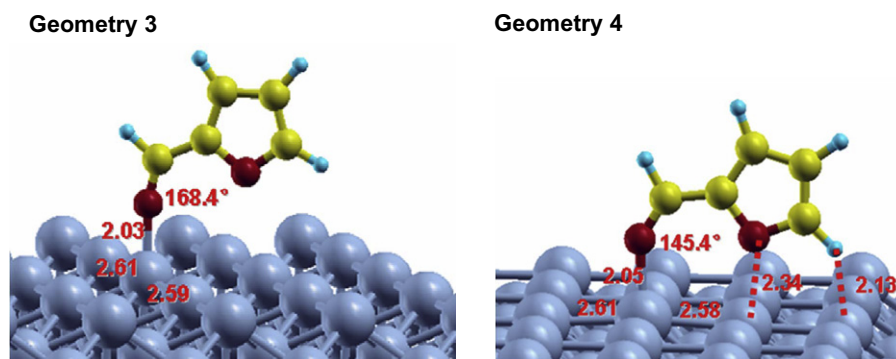


Fig. 15. Optimized geometries for adsorption configuration on Cu(1 1 0) with higher adsorption energies. The distances shown in the figure are in Å. For other plausible geometries, see Supplementary data.

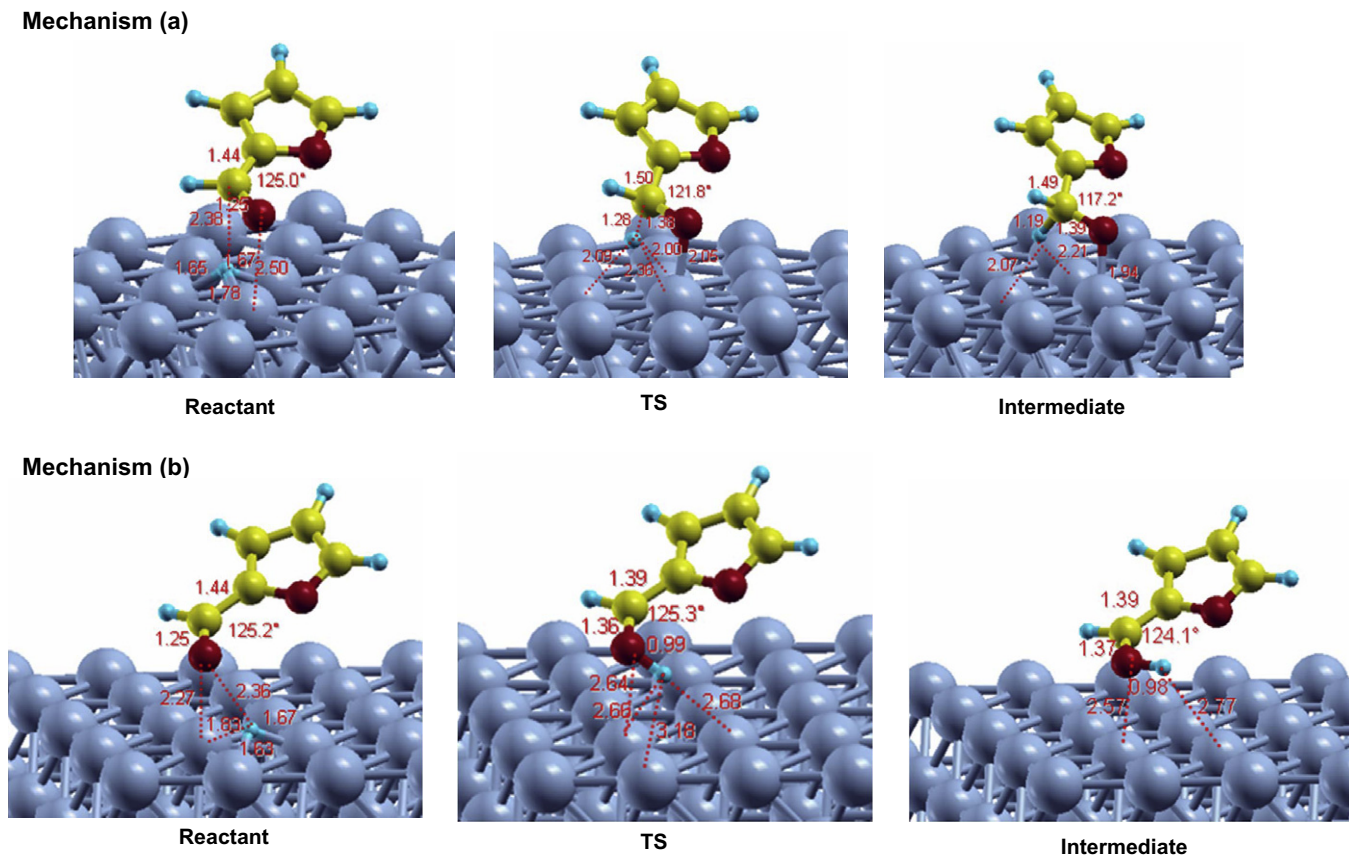


Fig. 16. Optimized geometries of the adsorbed furfural molecules, transition states, and intermediates Cu(1 1 1) via mechanisms (a) and (b). The distances shown in the figure are in Å.

with a reaction energy of 7.38 kcal/mol. The surface species, however, moves apart from the Cu(1 1 1) surface during the process. This may be explained by the hydrogen addition to the carbonyl O atom reducing the surface-O interaction. Notably, the C–C bond decreases from 1.44 Å to 1.39 Å in the hydroxylalkyl intermediate, whereas the bond length increases in the alkoxide intermediate. The C–C bond in furfural is shorter than a normal C–C single bond due to the delocalization of π electrons. The conjugation effect ceases after the hydrogen atom in addition to the carbonyl C in the alkoxide species, leading to a longer C–C bond. In the hydroxylalkyl species, the unpaired electron on the carbonyl carbon atom delocalizes to the aromatic ring and thus strengthens the C–C bond.

4. Discussion

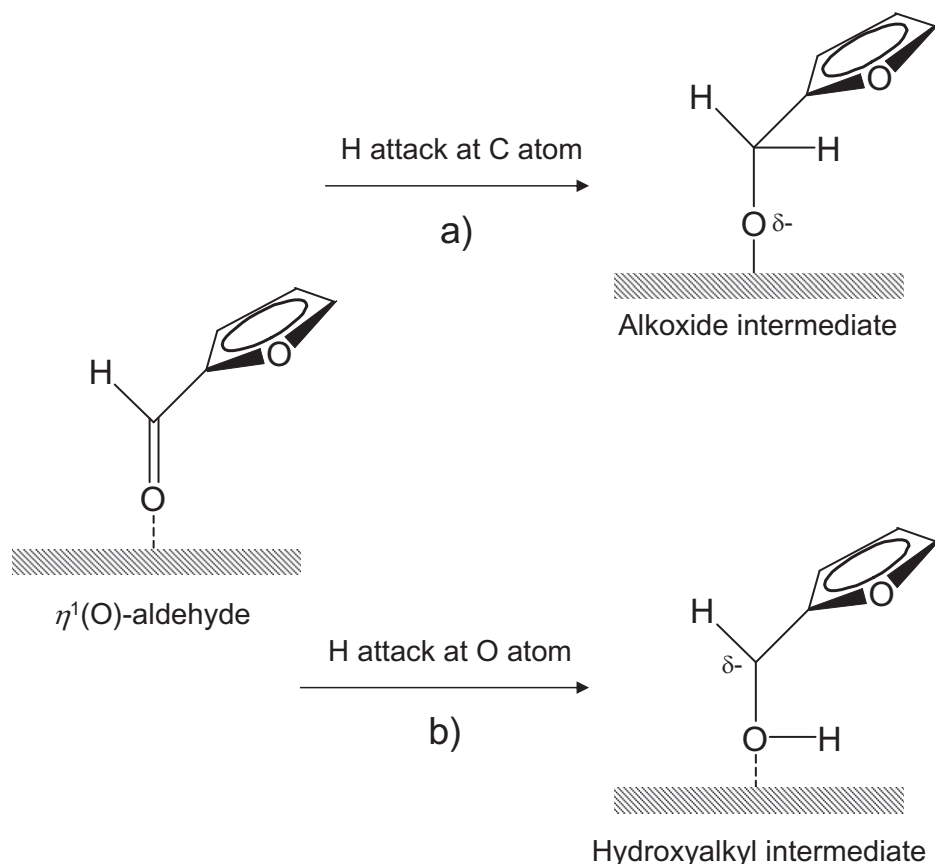
The hydrogenation of furfural on Cu yields furfuryl alcohol at high selectivity. Our combined experimental and theoretical studies indicate that the molecularly adsorbed furfural interacts with the Cu surface via the lone pair of oxygen to produce $\eta^1(\text{O})$ -aldehyde species. This intermediate then becomes a precursor for the hydrogenation reaction. While the di-sigma complex $\eta^2\text{-(C=O)}$ aldehyde could also be a precursor for hydrogenation [64], our DRIFTS results suggest that furfural adsorbs via the carbonyl O atom. Similarly, our DFT calculations show that the carbonyl perpendicular mode (O on top) is preferred on both Cu(1 1 1) and (1 1 0). The calculated adsorption enthalpies are in reasonable agreement with the fitting values obtained from kinetics model. The interaction between C and Cu atoms surface is relatively weak. There is a tendency of the adsorbed aldehyde to shift the C atoms away from the surface, even when both the C and O atoms were placed close to the sur-

face in the initial configuration. That is, the $\eta^2(\text{C=O})$ aldehyde, commonly observed on other metals (e.g. Pd, Pt), is not preferred on the Cu surface. The DFT calculations also give evidence for a repulsion of the furan ring from the Cu(1 1 1) surface, presumably due to the overlap of the 3d band of the surface Cu atoms and the anti-bonding orbital of the aromatic furan ring. On the Cu(1 1 0), the furan ring comes closer to the surface because a lower density of Cu atoms is involved in the interaction with the aromatic ring.

It is interesting to contrast the molecular interactions occurring on Cu with those on noble metals. For example, as opposed to Cu, Pd is known to adsorb the furan ring rather strongly due to a sp^2 -to- sp^3 rehybridisation [48,49]. A similar comparison can be made with the interaction of a molecule such as crotonaldehyde, which contains a carbonyl and a C=C bond. Analogous to the behavior shown here for furfural, it has been shown that on the Cu(1 1 1) surface, crotonaldehyde is bonded to the surface through the carbonyl O atom, with the C=C bond remaining largely unaffected and away from the surface [63]. By contrast, on Pt(1 1 1), the adsorption includes both C=O and C=C groups, with formation of $\eta^2(\text{C,O})$ and di- σ_{CC} , respectively [64].

To analyze the hydrogenation reaction pathway on Cu, one can start with the $\eta^1(\text{O})$ species. Two possibilities for the first attack by a H atom to the carbonyl group have been considered in the present contribution. The corresponding surface intermediates adsorbed on the surface are shown below:

Based on the DFT calculations, a first H attack to the O atom of the carbonyl that results in the formation of a hydroxylalkyl species (mechanism b) would have a lower energy barrier than a first H attack to the C atom of the carbonyl, which would lead to the formation of an alkoxide intermediate (mechanism a). The difference in stability between the two intermediates can be ascribed to the sta-



bilization role played by the aromatic furan ring. The addition of the first H atom to the O atom produces an unpaired electron on the C atom, which can be delocalized by the furan ring, which favors the formation of the hydroxyalkyl intermediate.

A similar concept can be applied to explain the higher stability of the hydroxyalkyl intermediate compared to the alkoxide intermediate in the hydrogenation of unsaturated aldehydes on Pt(1 1 1) [29–31]. In that case, the conjugation with the C=C bond would be expected to lower the energy barrier for the H attack at the O atom.

5. Conclusions

The conversion of furfural on Cu/SiO₂ yields mainly furfuryl alcohol from hydrogenation of the carbonyl, with only small amounts of 2-methylfuran, obtained from a subsequent cleavage of the C–O bond in furfuryl alcohol. A kinetic model for furfuraldehyde conversion has been developed based on a Langmuir–Hinshelwood model. The results from the fitting show a good agreement with experimental data obtained independently and the model shows to be valid when different mixtures are used as a feed, including the addition of water. Water is found to suppress furfural conversion, particularly at low temperatures. The physical parameters obtained from the fitting (heat of adsorption and activation energies) are in line with values previously reported in the literature. The rate constant for the hydrogenation of furfuraldehyde (k_1) is significantly higher than that for hydrodeoxygenation of furfuryl alcohol (k_2) to produce 2-methyl furan. The heat of adsorption (ΔH_{ads}) for furfural (12.3 kcal/mol) is similar to that of adsorption of water (12.4 kcal/mol), but higher than those for furfuryl alcohol (6.9 kcal/mol) and 2-methyl furan (3.7 kcal/mol). Moreover, the heat of adsorption of furfural is in agreement with

the adsorption energy predicted by the DFT calculations using a Cu(1 1 0) surface (7.3 kcal/mol).

The DRIFTS and DFT results demonstrate that the adsorption of furfural takes place preferentially in a $\eta^1(\text{O})$ -aldehyde (perpendicular) binding mode. Two possible mechanisms for furfuraldehyde hydrogenation have been compared, based on the order of the first H atom attack to the carbonyl group, resulting in two possible surface intermediates adsorbed on the Cu surface. The activation energy barrier for the first H addition to the O carbonyl group to form adsorbed hydroxyalkyl intermediates was found to be lower than when the first addition of H is to the carbonyl C forming an alkoxide intermediate (i.e., 7.6 kcal/mol compared to 10.8 kcal/mol). These results suggest that the presence of the aromatic furan ring helps stabilizing the hydroxyalkyl intermediate, lowering the energy barrier for this path.

Acknowledgments

This work was partially supported by the National Science Foundation EPSCOR (Grant 0814361), the Oklahoma Bioenergy Center, and the Department of Energy (Grant DE-FG36G088064). Computational resources from Texas A&M University Supercomputer center, from the National Energy Research Scientific Computing Center, which is supported by the Office of Science of the US Department of Energy under Contract No. DE-AC03-76SF00098, and from the University of Texas at Austin TACC system are gratefully acknowledged.

Appendix A. Supplementary data

Supplementary data associated with this article can be found, in the online version, at doi:10.1016/j.jcat.2010.10.005.

References

- [1] R.M. West, Z.Y. Liu, M. Peter, J.A. Dumesic, *Sustain. Chem.* 1 (2008) 417.
- [2] R. He, X.P. Ye, B.C. English, J.A. Satrio, *Bioresour. Technol.* 100 (2009) 535.
- [3] J. Adam, M. Blazso, E. Meszaros, M. Stocker, M.H. Nilsen, A. Bouzgac, J.E. Hustada, M. Gronli, G. Oyed, *Fuel* 84 (2005) 1494.
- [4] A. Demirbas, *Fuel Process. Technol.* 88 (2007) 591.
- [5] V.R. Wiggers, A. Wisniewski, L.A.S. Madureira, A.A. Chivanga Barros, H.F. Meier, *Fuel Process. Technol.* 88 (2009) 2135.
- [6] M.G. Perez, J. Shen, X.S. Wang, C.Z. Li, *Fuel Process. Technol.* 91 (2010) 296.
- [7] J. Lede, F. Broust, F.T. Ndiaye, M. Ferrer, *Fuel* 86 (2007) 1800.
- [8] M. Asadullah, M.A. Rahman, M.M. Ali, M.S. Rahman, M.A. Motin, M.B. Sultan, M.R. Alam, *Fuel* 86 (2007) 2514.
- [9] O. Onay, O.M. Kockar, *Fuel* 85 (2006) 1921.
- [10] A. Zabaniotou, O. Ioannidou, V. Skoulou, *Fuel* 87 (2008) 1492.
- [11] R.E.H. Sims, W. Mabey, J.N. Saddler, M. Taylor, *Bioresour. Technol.* 10 (2010) 1570.
- [12] D.E. Resasco, S. Crossley, *AIChE J.* 55 (2009) 1082.
- [13] C.A. Fisk, T. Morgan, Y. Ji, M. Crocker, C. Crofcheck, S.A. Lewis, *Appl. Catal. A* 358 (2009) 150.
- [14] F.M. Mercader, M.J. Groeneveld, S.R.A. Kersten, N.W.J. Way, C.J. Schaverien, J.A. Hogendoorn, *Appl. Catal. B* 96 (2010) 57.
- [15] L. Baijuna, L. Lianhaia, W. Bingchuna, C. Tianxia, K. Iwatani, *Appl. Catal. A* 171 (1998) 117.
- [16] H.Y. Zheng, Y.L. Zhu, B.T. Teng, Z.Q. Bai, C. Zhang, H.W. Xiang, Y.W. Li, *Appl. Catal. A* 171 (1998) 117.
- [17] B.M. Nagaraja, A.H. Padmasri, P. Seetharamulu, K. Hari Prasad Reddy, B. David Raju, K.S. Rama Rao, *J. Mol. Catal. A* 278 (2007) 29.
- [18] M.S. Murthy, K. Rajamani, *Chem. Eng. Sci.* 29 (1974) 601.
- [19] W. Huang, H. Li, B. Zhu, Y. Feng, S. Wang, S. Zhang, *Ultrason. Sonochem.* 14 (2007) 67.
- [20] H.Y. Zheng, Y.L. Zhu, L. Huang, Z.Y. Zeng, H.J. Wan, Y.W. Li, *Catal. Commun.* 9 (2008) 342.
- [21] C.J. Barrett, J.N. Chheda, G.W. Huber, J.A. Dumesic, *Appl. Catal.* 66 (2006) 111.
- [22] J. Wu, Y. Shen, C. Liu, H. Wang, C. Geng, Z. Zhang, *Catal. Commun.* 6 (2005) 633.
- [23] H. Li, H. Luo, L. Zhuang, W. Dai, M. Qiao, *J. Mol. Catal. A* 203 (2003) 267.
- [24] J.K. Kijeński, P. Winiarek, T. Paryczak, A. Lewicki, A. Mikołajska, *Appl. Catal. A* 233 (2002) 171.
- [25] B.M. Nagaraja, A.H. Padmasri, B.D. Raju, K.S. Rama Rao, *J. Mol. Catal. A* 265 (2007) 90.
- [26] K.J. Jung, A. Gaset, J. Molineir, *Biomass* 16 (1998) 63–76.
- [27] R.D. Srivastava, A.K. Guha, *J. Catal.* 91 (1985) 254.
- [28] H.Y. Zheng, Y.L. Zhu, B.T. Teng, Z.Q. Bai, C.H. Zhang, H.W. Xiang, Y.W. Li, *J. Mol. Catal. A* 246 (2006) 18.
- [29] G.M.R. van Druten, V. Ponc, *Appl. Catal. A: Gen.* 191 (2000) 163.
- [30] N.V. Pavlenko, A.I. Tripol'skii, G.I. Golodets, *Kinet. Katal.* 30 (1989) 1192.
- [31] R. Alcalá, J. Greeley, M. Mavrikakis, J.A. Dumesic, *J. Chem. Phys.* 116 (2002) 8973.
- [32] R.J. Madon, M. Boudart, *Ind. Eng. Chem. Fund.* 21 (1982) 438.
- [33] G. Kresse, J. Furthmüller, *J. Phys. Rev. B* 54 (1996) 11169.
- [34] G. Kresse, J. Hafner, *J. Phys. Rev. B* 49 (1994) 14251.
- [35] G. Kresse, J. Hafner, *J. Phys. Rev. B* 48 (1993) 13115.
- [36] G. Kresse, J. Hafner, *J. Phys. Rev. B* 47 (1993) 558.
- [37] G. Kresse, J. Furthmüller, *Comput. Mater. Sci.* 6 (1996) 5.
- [38] G. Kresse, D. Joubert, *J. Phys. Rev. B* 59 (1999) 1758.
- [39] P.E. Bloechl, *J. Phys. Rev. B* 50 (1994) 17953.
- [40] J.P. Perdew, K. Burke, M. Ernzerhof, *Phys. Rev. Lett.* 77 (1996) 3865.
- [41] D.E. Gray (Ed.), *American Institute of Physics Handbook*, third ed., McGraw-Hill, NY, 1972.
- [42] G. Mills, H. Jonsson, G.K. Schenter, *Surf. Sci.* 324 (1995) 305.
- [43] H. Jonsson, G. Mills, K.W. Jacobsen, *Nudged Elastic Band Method for Finding Minimum Energy Paths of Transitions*, World Scientific, Singapore, 1998.
- [44] B.M. Reddy, G.K. Reddy, K.N. Rao, *Appl. Catal. A* 265 (2007) 276.
- [45] M.A. Natal Santiago, M.A. Sanchez-Castillo, R.D. Cortright, J.A. Dumesic, *J. Catal.* 193 (2000) 16.
- [46] R.M. Rioux, M.V. Vannice, *J. Catal.* 216 (2003) 362.
- [47] R. Rao, A. Dandekar, R.T.K. Baker, M.A. Vannice, *J. Catal.* 171 (1997) 406.
- [48] M.K. Bradley, J. Robinson, D.P. Woodruff, *Surf. Sci.* 604 (2010) 920.
- [49] M.J. Knight, F. Allegretti, E.A. Kroger, M. Polcik, C.L.A. Lamont, D.P. Woodruff, *Surf. Sci.* 602 (2008) 2524.
- [50] M.A. Vannice, in: *Kinetics of Catalytic Reactions*, Springer, 2005.
- [51] M.A. Vannice, S.H. Hyun, B. Kalpakci, W.C. Liauh, *J. Catal.* 56 (1979) 358.
- [52] R.C. Weast, in: *Handbook of Chemistry and Physics*, CRC press, 1975.
- [53] B. Wang, D.W. Goodman, G.F. Froment, *J. Catal.* 253 (2008) 229.
- [54] R. Shekhar, M.A. Barteau, R.V. Plank, J.M. Vohs, *J. Phys. Chem. B* 101 (1997) 7939.
- [55] J.L. Davis, M.A. Barteau, *J. Am. Chem. Soc.* 111 (1989) 782.
- [56] J.L. Davis, M.A. Barteau, *Surf. Sci.* 268 (1992) 11.
- [57] M. Mavrikakis, M.A. Barteau, *J. Mol. Catal. A: Chem.* 131 (1998) 135.
- [58] J. Fujiki, H.J. Fan, H.H. Hattori, K. Tajima, Y.S. Tsai, E. Furuya, *Sep. Purif. Technol.* 60 (2008) 223.
- [59] J.N. Kondo, E. Yoda, H. Ishikawa, F. Wakabayashi, K. Domen, *J. Catal.* 191 (2000) 275.
- [60] N.R. Avery, *Surf. Sci.* 125 (1983) 771.
- [61] L.E. Murillo, J.G. Chen, *Surf. Sci.* 602 (2008) 919.
- [62] J.L. Davis, M.A. Barteau, *Surf. Sci.* 235 (1990) 235.
- [63] M. Boronat, M. May, F. Illas, *Surf. Sci.* 602 (2008) 3284.
- [64] F. Delbecq, P. Sautet, *J. Catal.* 211 (2002) 398.